Spin-Polarized Positron Beams with ^{22}Na and ^{68}Ge and Their Applications to Materials Research

K. Wada, A. Miyashita, M. Maekawa, S. Sakai, A. Kawasuso [a)]

National Institutes for Quantum and Radiological Science and Technology, 1233, Watanuki, Takasaki, Gunma 370-1292 JAPAN

[a)]kawasuso.atsuo@qst.go.jp

Abstract. We introduce our research and development of spin-polarized positron beams with ^{22}Na and ^{68}Ge sources and their applications to spin-related materials research in the period of 2008 to 2017. We also discuss the prospects of spintronics study with spin-polarized positron spectroscopy.

INTRODUCTION

Positrons emitted from radioisotopes are longitudinally spin-polarized due to the parity non-conservation in the weak interaction [1-3]. After this discovery, using angular correlation of annihilation radiation (ACAR) technique, the investigation of ferromagnetic band structures had been started. However, in the late 1960, the other competitive tools, such as magnetic Compton profiling and photoemission electron spectroscopy, were developed one after another. Consequently, the study of magnetism with spin-polarized positron spectroscopy turned out to be minor.

In 1979, the role of spin-polarized positron spectroscopy was again paid the attention due to the invention of spin-polarized 'slow' positron beam by the Michigan group [4]. At that time, the surface physics was rapidly progressing accompanying the technological innovation such as ultra-high vacuum technology and the scanning tunneling microscopy. Novel phenomena were anticipated to occur at solid surfaces due to the dimension lowering. Magnetic dead layer hypothesis that means the disappearance of magnetic moment at surfaces of ferromagnets [5], was argued in such tendency. To confirm new hypothesis, the further development of experimental techniques were required. The spin polarization of the Michigan ^{58}Co-based beam was 22 %. They reported that, by rejecting low energy positrons from the source, the spin polarization could be enhanced to ~70 %. In 1982, they found that Ni surface is in magnetically 'live' layer against the dead layer hypothesis [6]. This demonstrated the superiority of spin-polarized slow positron beam in the study of surface magnetism. However, leaving this paper, no further researches had been conducted. From 1997 to 1999, the Tokyo Metropolitan University [7] and RIKEN [8] groups attempted to generate spin-polarized slow positron beams with ^{27}Si and ^{18}F sources.

Recently, towards the innovation of electronic devices by using electron charge and spin together, so-called spintronics research is brisk. The discovery of giant magnetoresistance giving rise to the tremendous increase of hard disk memory capacity is a representative outcome of the spintronics. Currently, half-metals that have ideally 100 % spin polarization at the Fermi level, and magnetic semiconductors in which the magnetism is controllable using electric field and light are extensively investigated. The further intriguing phenomena and materials, such as the spin-Hall effect, the Rashba effect, topological insulators and graphene-related monoatomic layer materials are also explored enthusiastically. Discovery of new phenomena and materials stimulates the development of more advanced new experimental techniques.

Taking advantage of the spin sensitivity of positron, the traditional positron spectroscopies will become state-of-the-art techniques. In light of the above-mentioned circumstances, the spin-polarized positron spectroscopy may be revived, improved and applied to the research of spintronics materials. In this article, we introduce our research and development of spin-polarized positron beam. We also discuss the prospects of this method including anticipation to the development of intense and highly spin-polarized positron beam.

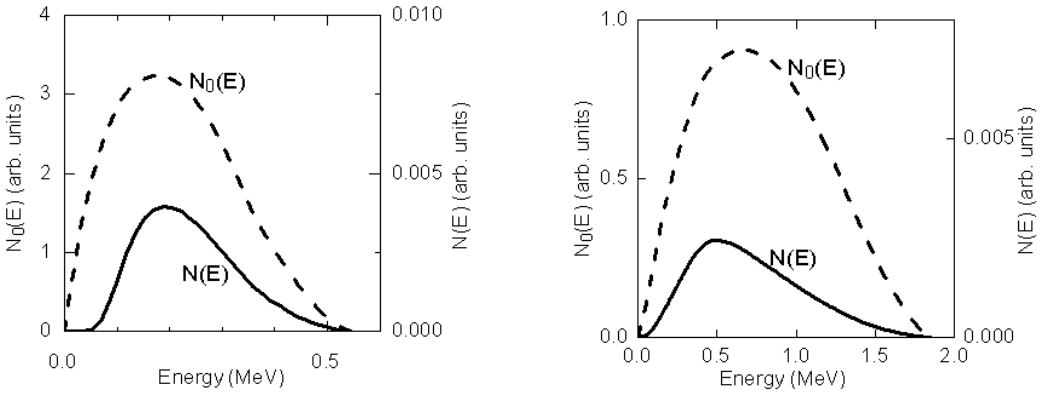

FIGURE 1. Intrinsic energy distribution of positrons, $N_0(E)$, and effective energy distribution of positrons converted to slow positrons from the source to the moderator, $N(E)$ for (a) ^{22}Na source of d_S=0.1 mm and (b) ^{68}Ge source of d_S=0.5 mm and with a tungsten moderator of d_M=1 μm and no absorber

DEVELOPMENT AND APPLICATION OF SPIN-POLARIZED POSITRON BEAM

Expected beam spin polarization

Longitudinal spin polarization of positrons emitted from radioisotopes (RIs) is given as the helicity (v/c), where v and c are the speeds of positrons and light, respectively. Since normally nuclear spins of radioisotopes are randomly oriented, positrons are isotropically (4π direction) emitted. Average spin polarization of positrons into a cone with an open angle of θ and in the energy range from E_1 to E_2 is given by

$$\langle P_+ \rangle = \frac{\langle v \rangle}{c}\frac{1+\cos\theta}{2} = \int_{E_1}^{E_2}\sqrt{1-\frac{1}{[1+E/(mc^2)]^2}}N(E)dE\frac{1+\cos\theta}{2},$$

where <v> and $N(E)$ are the average speed and the energy distribution, respectively, of positrons. From this, higher spin-polarization is obtained by using RIs with higher Q values, restricting the cone angle and backscattering, and selecting the higher energy component. If the nuclear spins can be aligned in one direction, both spin-polarization and emission probability to that direction can be enhanced simultaneously.

Spin polarization also depend on the details of experiment. Firstly, the effective energy distribution of positrons is no longer the same as the intrinsic one ($N_0(E)$) because of (i) the energy dependent absorption of positrons in the source material and the intentional absorber, (ii) the energy selection by the moderator for slow positron generation. Secondly, various depolarization effects should be considered. The major processes are (i) the backscattering of positrons by the source substrate and (ii) the spin-flipping during scattering processes in the moderator.

Let us assume that slow positrons are generated by a source-absorber-moderator alignment. The energy distribution of positrons that are moderated and reemitted as slow positrons may be given by

$$N(E) = \frac{1}{2}\int_0^{d_S} N_0(E)[A(z)/A_0]T_S(E,z)dz \times T_A(E,d_A)\times\varepsilon_M(E,d_M),$$

where z is the depth from the surface, $A(z)$ is the source activity (total amount of A_0 in d_s thick) distribution, $T_{S,A}(E, z)$ is the transmittance of positrons in the source and the absorber with d_A thick, and $\varepsilon_M(E, d_M)$ is the efficiency of moderator of d_M thick. Figure 1 shows $N_0(E)$ and $N(E)$ for ^{22}Na source of d_S=0.1 mm and ^{68}Ge source of d_S=0.5 mm with tungsten moderator of d_M=1 μm and no absorber (T_A=1). The spin polarizations after the moderation are 41% (^{22}Na) and 53% (^{68}Ge) with a realistic open angle $\theta = 78^o$ [9].

Backscattering processes of positrons that occur in the source-absorber-moderator component is very complicated, since the energy and angle dependent backscattering probability, the transmission after backscattering in the series of materials, and their multiple processes should be taken into account. Here, we simply assume that the backscattering by the source substrate is the major depolarization process. The backscattering probability for ^{22}Na and ^{68}Ge on a Z material is given empirically as R = 0.342log Z – 0.146 [10]. Assuming that positrons with any angles and energies are backscattered at a carbon substrate (Z=6), R~10 % and hence 10 % polarization will be lost.

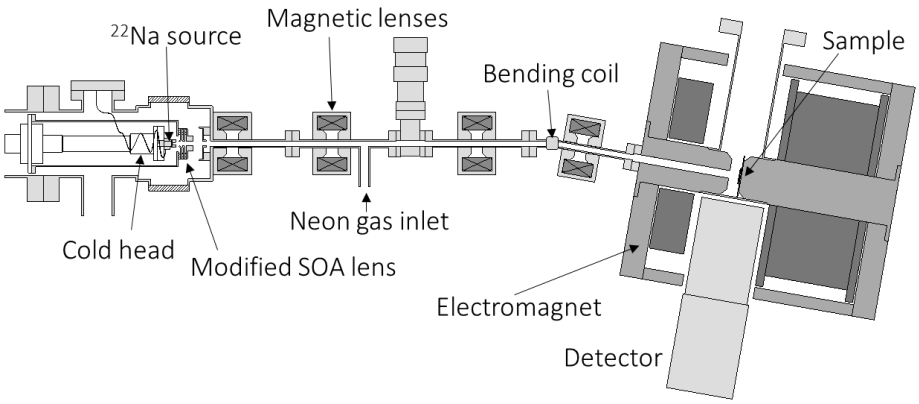

(a)

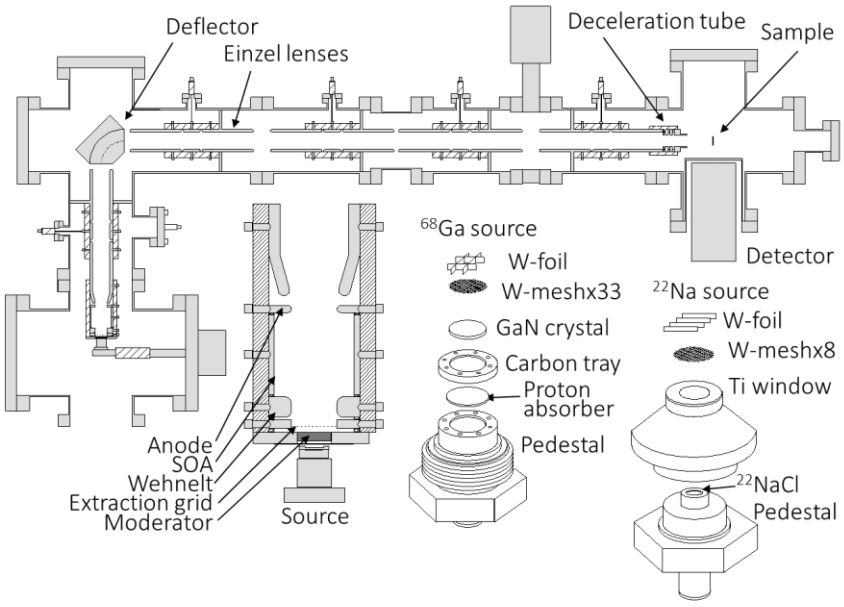

(b)

FIGURE 2. Slow beam apparatuses with ^{22}Na and ^{68}Ge sources developed by the authors: (a) Electromagnetic beam and (b) Electrostatic beam

Interaction between positrons and materials may be classified into the electromagnetic interaction (bremsstrahlung and Bhabha scattering), dielectric interaction (electron-hole and plasmon excitations), phonon excitation and elastic Mott-Coulomb scattering. The stopping power of the bremsstrahlung is *EZ*/800 of that of the Bhabha scattering and hence it is not so important in the case of RI positrons. Positrons injected into a material lose the most of energy through the ionization of the Bhabha scattering. When the energy reaches ~keV range, the electron-hole and plasmon excitations become major energy loss processes. In ~eV range, positrons are thermalized through the phonon excitation. During the above slowing-down processes, in the Bhabha scattering, positron spins are flipped. In the quantum electromagnetic dynamics theory, the spin-flipping probability of positron is given as a function of positron energy and the energy transfer [11]. From $N(E)$ in Fig. 1, the mean positron energies, that are converted to slow positrons from ^{22}Na and ^{68}Ge sources, are ~0.2 MeV and ~0.7 MeV, respectively. The mean energy transfer per scattering is ~500 eV in tungsten [12]. The spin-flipping probabilities are approximately 3×10^{-4} (^{22}Na) and 8×10^{-5} (^{68}Ge) per scattering. About 400 (^{22}Na) and 1400 (^{68}Ge) scattering events may occur until zero energy. Thus, about 6% (^{22}Na) and 5 % (^{68}Ge) polarizations may be lost. In the Mott scattering, due to the spin-orbit interaction, spin is rotated to the direction of scattering. For electron, the depolarization amount is given as an

analytical formula [13]. Assuming that it is applicable to positron, too, 5% (^{22}Na) and 3 % (^{68}Ge) polarizations may be lost in the tungsten moderator with d_M=1 μm.

Thus, in total, the spin polarizations of slow positron beams may be 41 % (absorption) ×0.9 (backscattering) ×0.94 (Bhabha) ×0.95 (Mott) = 33 % (^{22}Na) and 53 % (absorption) ×0.9 (backscattering) ×0.96 (Bhabha) ×0.95 (Mott) = 43 % (^{68}Ge). No significant depolarization occurs as long as light materials are used as source substrate. Use of absorber will enhance the final spin polarization.

Examples of beam apparatus

Spin-polarized positron beam can be generated with RIs and no special devices. The simplest way may be direct injection of fast positrons emitted from the source into the sample without moderation. This method may be suited for out-of-plane magnetized bulk ferromagnets [14, 15]. The authors developed slow beam apparatuses with ^{22}Na and ^{68}Ge sources as shown in Fig. 2 [16, 17]. The apparatus of Fig. 2(a) is based on electromagnetic lenses. In this method, the beam direction and the field direction of beam focusing are the same and hence the longitudinal spin polarization is conserved well. Relatively strong magnetic field (~a few Tesla) can be applied to the sample. The apparatus of Fig. 2(b) is based on electrostatic lenses. By bending the beam 90^o by an electrostatic deflector, transversely spin-polarized beam is obtained.

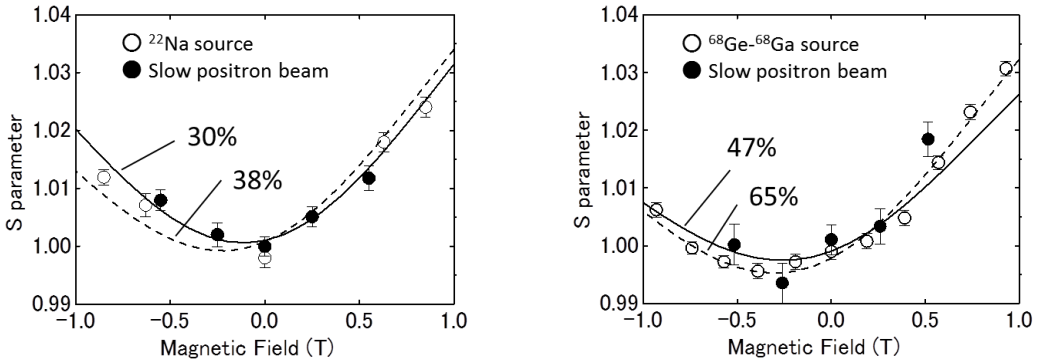

(a) (b)

FIGURE 3. DBAR *S* parameter in a fused silica obtained using (a) ^{22}Na source itself and its electrostatic beam and (b) ^{68}Ge source itself and its electrostatic beam as a function of magnetic field. The evaluated spin polarizations are also shown

Measurement of spin-polarization with positronium

Positron spin-polarization can be measured through the spin-dependent transmission into ferromagnets and the Mott scattering by gold target. After the Michigan group [4], the method using the magnetic quenching of positronium is also available. We determined the spin-polarization of our beams by the Nagai's method based on the positronium magnetic quenching in fused silica [18]. In this method, the spin polarization is determined using the fact that the *S* parameter of the Doppler broadening of annihilation radiation (DBAR) spectrum is the first order function of the two-photon annihilation intensity in magnetic field. That is, the magnetic field dependence of *S* parameter is given by

$$S = (S_{Ps} - S_{SiO_2})I(B) + S_{SiO_2} = (S_{Ps} - S_{SiO_2})\left(\frac{F_{|00\rangle'}}{\lambda_{|00\rangle'}}\frac{\kappa\lambda_p}{1+y^2} + \frac{F_{|10\rangle'}}{\lambda_{|10\rangle'}}\frac{\kappa y^2\lambda_p}{1+y^2}\right) + S_{SiO_2}\,.$$

Here, S_{Ps} is the *S* parameter of self-annihilation of perturbed positronium, S_{SiO2} is the *S* parameter of other two-photon annihilation events, $I(B)$ is the fraction of perturbed positronium as a function of magnetic field, $F_{|00>'}$ and $F_{|10>'}$ are the fractions of perturbed para- and ortho-positronium, respectively, λ_p, $\lambda_{|00>'}$, $\lambda_{|10>'}$ are the annihilation rates of para-, perturbed para- and ortho- positronium, respectively, $y=x/[(1+x^2)^{1/2}+1]$, $x=4\mu_B B/\Delta E$ (μ_B: Bohr magneton, B: magnetic field, ΔE: hyperfine interaction energy (8.4×10^{-4}eV) and κ is the contact density which is the ratio of square of positronium wave-functions in materials and vacuum ($=|\Psi_m(0)|^2/|\Psi_v(0)|^2$). By fitting the above equation to experimental field dependence of *S* parameter, P_+ is obtained. The details are described elsewhere [9].

Figure 3 shows the magnetic field dependences of *S* parameter in a fused silica by directly implanting fast positrons from ^{22}Na and ^{68}Ge sources and by the slow positrons. The separation between the sample and the source is 7 mm. By the above-mentioned Nagai's method, the spin-polarizations are determined to be 38 % (^{22}Na) and 65 % (^{68}Ge) for fast positrons and 30 % (^{22}Na) and 47 % (^{68}Ge) for slow positrons. These values agree well with those estimated in the previous subsection.

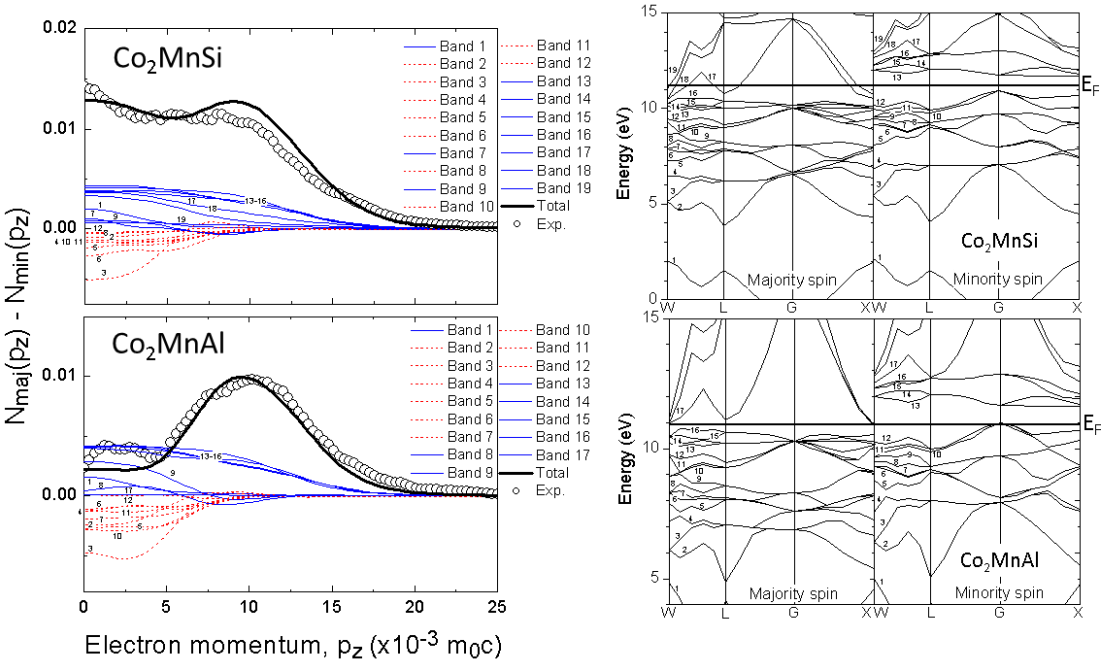

FIGURE 4. (Left): Differential DBAR spectra between majority and minority spin bands obtained for Co_2MnSi (CMS) and Co_2MnAl (CMA). Right: Band structures of CMS and CMA calculated by the ABINIT code

Application of spin-polarized positron spectroscopy

Ferromagnetic band structure

Here, as an example, we pick up the Heusler alloys. Some of the Heusler alloys are thought to be half-metals. Half-metal is a metal having a gap in either majority or minority spin bands, i.e., ideally 100 % spin-polarization at the Fermi level. Because of this novel property, half-metals are extensively studied in spintronics as promising materials to give rise to very large magnetoresistance. Spin-polarized positron spectroscopy based on ACAR and DBAR spectra may be useful to examine the ferromagnetic band structures and hence the half-metallicity.

As shown in Fig. 4 (left), for two Heusler alloys (Co_2MnSi (CMS) and Co_2MnAl (CMA)) that are expected to be half-metals, we obtained the differential DBAR spectra between majority and minority spin bands, which is directly comparable to theoretical calculation, as

$$N^{maj}(p_z) - N^{\min}(p_z) = [N_+(p_z) - N_-(p_z)] + P_+[(\lambda^{\uparrow} - \lambda^{\downarrow})/(\lambda^{\uparrow} + \lambda^{\downarrow})][N_+(p_z) + N_-(p_z)],$$

where $\lambda^{\uparrow(\downarrow)}$ is the annihilation rate of spin up (down) positrons, and $N_{\pm}(p_z)$ is the DBAR spectrum in positive and negative magnetic field [19]. For the CMS sample, a bump at around p=0 m_0c and a shoulder at around p=10 m_0c are seen. For the CMA sample, the intensity at around p=0 m_0c is significantly lost. Contrarily to the CMS sample having $L2_1$ structure, the CMA sample was in fully disordered B2 structure. Therefore, one may consider that the reduced intensity of the CMA sample at around p=0 m_0c is due to the B2 disordering. Furthermore, the above difference between the CMS and CMA samples may be correlated with the general trend that CMS has a higher half-metallicity as compared to CMA. However, the above argument is not true as explained below. The solid lines in Fig. 4 are theoretical curves assuming $L2_1$ structure. The blue (thin solid) and red (broken) lines represent positive and negative polarizations, respectively. Agreement between experiment and theory is good even if the CMA

sample was in fully B2 structure. This indicates that the band structure and hence the electron momentum distribution is not dramatically changed between $L2_1$ and B2 structures. Actually, our calculation supported this assumption. The bump at around p=0 m_0c and the shoulder at around p=10 m_0c for the CMS sample are interpreted as that, the total intensity of the positively polarized 17 th to 19 th bands having *sp*-like dispersion and the 13 th to 16 th bands having *d*-like dispersion overcompensate the total intensity of the other negatively polarized bands. In the case of CMA, the 13 to 16 th bands are similarly positively polarized, but, the 17 th to 19 bands have nearly no states. Consequently, their total intensity does not exceed the total intensity of the other negatively polarized bands and hence the valley at around p=0 m_0c appears. As seen from the calculated band structures in Fig. 4 (Right), CMS has theoretically better half-metallicity as compared to CMA. Thus, considering the above arguments, it is concluded that, (i) from the agreement between experiment and theory, the CMS sample has a higher half-metallicity than the CMA sample and (ii) the half-metallicity is robust for the disordering from $L2_1$ to B2 structures.

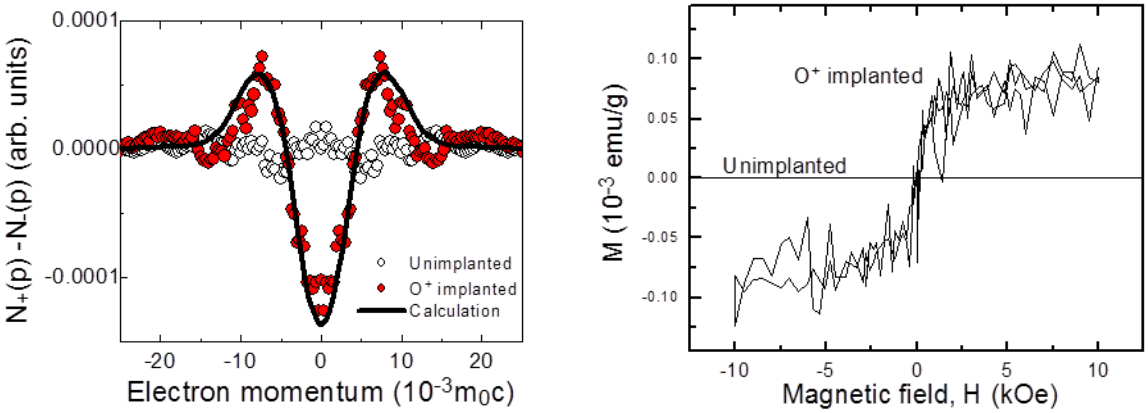

FIGURE 5. (a) Differential DBAR spectra in positive and negative magnetic fields and (b) the M-H curve, obtained for a hydrothermally-grown ZnO before and after oxygen irradiation ZnO. Sold line in (a) is the theoretical DBAR spectrum for electrically neutral zinc vacancy

Vacancy-induced ferromagnetism

It is demonstrated that ferromagnetism appears in originally non-magnetic materials without intentional doping of magnetic elements. Many subsequent investigations demonstrated that such ferromagnetism is a common feature of metal oxides, nitrides and carbides. Zinc oxide (ZnO), which is a wide-bandgap semiconductor, is one of such materials. The origin of the ferromagnetism is speculated to be due to atomic vacancies. However, no direct evidences for this speculation have been obtained. Since positrons are preferentially trapped by atomic vacancies in solids, spin-polarized positron spectroscopy may be a powerful tool to confirm the existence of magnetic moments at vacancies, i.e., vacancy-induced ferromagnetism.

Figures 5(a) and 5(b) show the differential DBAR spectra in positive and negative magnetic fields and the M-H curve, respectively, obtained for a hydrothermally-grown ZnO before and after oxygen irradiation [20]. After oxygen irradiation, the DBAR spectrum shows clear field reversal symmetry. The M-H curve also shows a ferromagnetic history. After oxygen irradiation, most of positrons get trapped by zinc vacancies. The solid line in Fig. 5(a) is the calculated differential DBAR spectrum for electrically neutral zinc vacancies. It reproduces the experiment quite well. The finite differential intensity is due to the high spin state associated with zinc vacancies. For oxygen vacancies and nearest neighbor divacancies, no differential curves (only horizontal lines) are obtained. The above results allow us to conclude that electrons at zinc vacancies are spin-polarized contributing to the macroscopic ferromagnetism.

There are many other potential candidates of vacancy-induced ferromagnetism such as doped or irradiated GaN, AlN, SnO_2, CeO_2, etc. Spin-polarized positron spectroscopy may also be applied to these systems. Development of spin-polarized positron lifetime spectroscopy will be more helpful to promote this kind of studies.

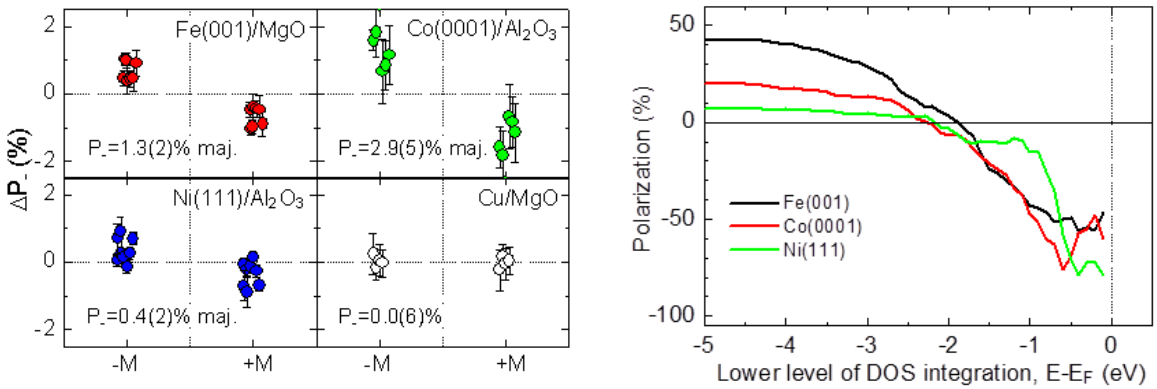

(a) (b)

FIGURE 6. (a) Surface spin polarizations observed for bcc-Fe(001)/MgO(001), hcp-Co(0001)/Al_2O_3(0001), fcc-Ni(111)/Al_2O_3(0001) and polycrystalline Cu/MgO(001). $\pm$M denotes that the magnetization of sample is parallel (antiparallel) to the positron spin polarization. (b) Theoretical spin polarizations of the vacuum region of Fe(001), Co(0001) and Ni(111) surfaces as a function of the lower energy level of density of states. That is, positrons are assumed to pick-up electrons from the lower level to E_F

Surface spin polarization

In spintronics, surface and interface are extremely important concerning spin injection into non-magnetic layer from ferromagnetic substrate, and spin current/accumulation induced via strong spin-orbit interaction. That is, surface spin polarization should be evaluated with less disturbances from deep layers. However, conventional methods such as photoemission spectroscopy and magneto-optical effect measurement are not necessarily sufficient for the above requirements. Spin-polarized positron spectroscopy based on surface positronium formation will be an alternative method since positronium is assured to be formed at the first surface layer. When both positrons and electrons are spin-polarized, from the change of positronium intensity upon spin reversal, surface spin polarization can be obtained [6].

Figure 6(a) shows the spin polarizations obtained for clean bcc-Fe(001)/MgO(001), hcp-Co(0001) and fcc-Ni(111) on Al_2O_3(0001) and polycrystalline Cu/MgO(001) with the film thicknesses of 30-100 nm. The spin polarization of the Cu sample is under the detection limit, while all the other samples exhibit finite spin polarizations. From the signs of the spin-polarizations, majority spin electrons are detected. Figure 6(b) shows the calculated spin polarizations in the vacuum regions of Fe(001), Co(0001) and Ni(111) surfaces as a function of lower energy level of integration below the Fermi level. From this, if electrons located only above E_F-1.5 eV are picked-up by positrons, the observation of majority spins is not explained. Probably, positrons pick up electrons in deeper levels, too.

We have also evaluated the surface spin polarizations induced on metals known as spin-Hall and Rashba systems [21-23]. The topological insulators and graphene-related monoatomic layer materials are also the potential applications. For more quantitative discussion, positronium formation mechanisms should be revealed both in experiment and theory. Spin-, energy- and angle-resolved positronium spectroscopy is required ultimately.

PERSPECTIVE OF SPIN-POLARIZED POSITRON SPECTROSCOPY

Early studies of ferromagnetic band structures were performed with ACAR method. Though ACAR is useful for the Fermi surface mapping, at present, only bulk study is possible since slow positron beams with enough intensity (>10^9 e^+/sec) and spin polarization (>50 %) have not yet been in use. We demonstrated that DBAR method can also be used for studying ferromagnets. This measurement is possible even with low beam flux (10^4-10^5 e^+/sec) from RI sources. Also, magnetic moments of vacancies in thin films and subsurface regions can be detected. Spin-polarized and pulsed positron beam may also be a powerful probe for detecting magnetic moments of vacancies, since lifetime spectroscopy provides more direct information about open volumes and electron densities associated with vacancies.

For the study of surface spin polarization, currently, only a simple positronium spectroscopy (gamma-ray energy and lifetime measurements) is available. This method has an advantage about selectivity of the first surface layer that the other methods are hardly accessible. But, to deduce more detailed information about spin-polarized

electronic state, energy- and angle-resolvability is also required. If the surface positronium spectroscopy with spin, energy and angle resolutions is realized, it is possible to determine spin polarization at the Fermi level, spin-polarized density of states and band dispersion that are practically of importance. We may call this technique "spin and angle-resolved positronium spectroscopy". Surface spin polarization can also be studied through positron surface state since it has characteristic long lifetimes (>500 ps) which is distinguishable from bulk annihilation. For doing this, spin-polarized and pulsed positron beam is again needed.

The above experiments can be conducted somehow even using RI-based beams. But, as mentioned above, in ACAR experiments of thin films, spin-polarized 'intense' beam is absolutely needed. This may be difficult with RIs. Spin-polarized intense positron beam can open other possibilities, too, such as micro-probing of spin polarization. Obviously, higher beam spin polarization gives better results in spin-polarized positron spectroscopy experiments. Beam intensity of 10^{10} e^{+}/sec plus spin-polarization of more than 90 % would be an ultimate goal of positron beam development.

ACKNOWLEDGMENTS

This work was partly supported by JSPS KAKENHI under Grant No. 24310072, 15K14135, 17K19061.

REFERENCES

1. C. S. Wu, E. Ambler, R. W. Hayward, D. D. Hoppes, R. P. Hudson, Phys. Rev. **105**, 1413-1415(1957).
2. T. D. Lee, C. N. Yang, Phys. Rev. **104**, 254-258(1956).
3. S. S. Hanna and R. S. Preston, Phys. Rev. **106**, 1363-1364(1957).
4. P. W. Zitzewitz, J. C. Van House, A. Rich and D. W. Gidley, Phys. Rev. Lett. **43**, 1281-1284(1979).
5. L. M. Liebermann, D. R. Fredkin and H. B. Shore, Phys. Rev. Lett. **22**,539-541(1969), L. M. Liebermann, J. Chilton, D. M. Edwards, J. Mathon, Phys. Rev. Lett. **25**,232-235(1970).
6. D. W. Gidley and A. R. Koymen, Phys. Rev. Lett. **49**, 1779-1783(1982).
7. T. Kumita, M. Chiba, R. Hamatsu, M. Hirose, T. Hirose, H. Iijima, M. Irako, N. Kawasaki, Y. Kurihara, T. Matsumoto, H. Nakabushi, T. Omori, Y. Takeuchi, M. Washio and J. Yang, Appl. Surf, Sci. **116**, 1-6(1997).
8. F. Saito, T. Hyodo, Y. Nagashima, T. Kurihara, N. Suzuki, Y. Itoh, and A. Goto, "Intense Radioisotope Sources for Spin Polarized Positron Beams" in *New Directions in Antimatter Chemistry and Physics*, edited by C. M. Surko and F. A. Gianturco (Kluwer Academic Publishers, The Netherlands, 2001)pp.35-45.
9. M. Maekawa, Y. Fukaya, A. Yabuuchi, I. Mochizuki, A. Kawasuso, Nucl. Inst. Meth. Phys Res. B**308**, 9-14(2013).
10. I. K. MacKenzie, C. W. Shulte, T. Jackman and L. Campbell, Phys. Rev. **A7**, 135-145(1973).
11. C. K. Iddings, G. L. Shaw and Y. S. Tsai, Phys. Rev. **135**, B1388-B1397 (1964).
12. R. M. Sternheimer, Phys. Rev. B **103**, 511-515(1956).
13. M. E. Rose and H. A. Bethe, Phys. Rev. **55**, 277-289(1939).
14. A. Kawasuso, M. Maekawa, Y. Fukaya, A. Yabuuchi, and I. Mochizuki, Phys. Rev. B **83**, 100406(R) (2011), Phys. Rev. B**83**, 100406(R)-1-3(2011).
15. A. Kawasuso, M. Maekawa, Y. Fukaya, A. Yabuuchi and I. Mochizuki, Phys. Rev. B**85**, 024417-1-6(2012).
16. M. Maekawa, Y. Fukaya, H. Zhang, H. Li and A. Kawasuso. J. Phys.: Conf. Ser., **505**, 012033-1-4(2014).
17. M. Maekawa, H. Zhang, H. Li, Y. Fukaya, A. Kawasuso, Jpn. J. Appl. Phys. Conf. Proc. **2**, 011305-1-6(2014).
18. Y. Nagai, Y. Nagashima, J. Kim, Y. Itoh, and T. Hyodo, Nucl. Instrum. Meth. Phys. Res. B **171**, 199-203(2000).
19. H. Li, M. Maekawa, A. Miyashita, A. Kawasuso, Defect and Diffusion Forum, **373**, 65-70 (2016).
20. M. Maekawa, H. Abe, A. Miyashita, S. Sakai, S. Yamamoto, A. Kawasuso, Appl. Phys. Lett., **110**, 172402-1-5(2017).
21. A. Kawasuso, Y. Fukaya, M. Maekawa, H. Zhang, T. Seki, T.Yoshino, E. Saitoh, K. Takanashi, J. Mag. Mag. Mater. **342,** 139-143(2013).
22. H. J. Zhang, S. Yamamoto, Y. Fukaya, M. Maekawa, H. Li, A. Kawasuso, T. Seki, E. Saitoh& K. Takanashi, Scientific Reports **4,** 04844-1-5(2014).
23. H. J. Zhang, S. Yamamoto, B. Gu, H. Li, M. Maekawa, Y. Fukaya, and A. Kawasuso Phys. Rev. Lett. **114**, 166602-1-5(2015).